International Journal of Innovative Computing, Information and Control
Volume **9**, Number **8**, August **2013**

ICIC International ©2013 ISSN 1349-4198
pp. 3357–3376

CIRCULATING FLUIDIZED BED HOT-LOOP ANALYSIS, TUNING, AND STATE-ESTIMATION USING PARTICLE FILTERING

Enso Ikonen[1,*], Jenő Kovács[1] and Jouni Ritvanen[2]

[1]Systems Engineering Laboratory
Department of Process and Environmental Engineering
University of Oulu
POB 4300 FIN-90014 University of Oulu, Oulu, Finland
*Corresponding author: enso.ikonen@oulu.fi; jeno.kovacs@oulu.fi

[2]Faculty of Technology
Lappeenranta University of Technology
Lappeenranta, Finland
jouni.ritvanen@lut.fi

Received June 2012; revised October 2012

Abstract. *Analysis, tuning and state estimation of an industrial process based on a physical model and experimental data are considered. Selected model outputs are fitted to measured data by allowing a set of constant-valued parameters to vary with time. Particle filters provide a Bayesian approach to parameter/state estimation, utilizing both the system model and measured data. The main aim of the work is to examine the possibilities of developing an engineering tool for testing and/or extracting useful hypotheses during examination of a dynamic test period outcomes. An approach based on particle filtering techniques is suggested. Other applications of the developed tools are proposed in model tuning and on-line monitoring of plant state. An illustrative case study is presented, using data and model for a full scale power plant. The case example considers a circulating fluidized bed (CFB) combustion process, for which a hot-loop model has been developed. Time-varying values for heat transfer and fuel moisture parameters, together with the associated uncertainties, are estimated using particle filters. The performance of the approach with real, industrial data and a full-scale model was found promising.*
Keywords: Bayesian reasoning, Power plants, Process engineering, Smoothing

1. **Introduction.** A large amount of modeling work is conducted at the industry and academia to model various industrial processes. A major use of the industrial plant models is in the analysis of the operation and performance of the process. A what-if analysis might include examination of variable and parameter sensitivities, and relative importance of various parameters and/or system components. Data records are continuously collected from most modern industrial processes, due to various reasons such as economical assessments, production planning, environmental regulations. Coherence between simulated model outcomes and plant data increases our belief that the explanation mechanisms provided by the model are correct. Deviations between simulations and data may be due to problems in the model (e.g., incorrect model components, missing components, inappropriate parameter values), inaccuracies with the measurements (systematic errors in measurement due to measurement malpositioning, wearing, fouling, etc.), or unmeasured disturbances during the process experiments (variations in raw material quality, load changes, etc.), etc. A common approach in fault diagnosis [15] is to compare the error residuals, between measured data and corresponding data simulated using a model or a bank of models for a number of priori determined scenarios. The former enables to

detect if a fault has occurred, while the latter attempts also to identify the fault, such as equipment failure or leakage.

Nowadays, dynamic process models are quite commonly used to develop control systems and to analyze the dynamic behavior of various types of boilers and power plants [27]. The models utilized in control design traditionally have relatively simple structures, sets of linear time-invariant transfer functions or linear/non-linear state-space models are often used. On the other hand, the dynamic models used in process design and development, including the process know-how, are almost invariably based on phenomenological relations (physical and chemical phenomena) completed with experimental correlations. The iterative evolvement of such models is illustrated in Figure 1. The two main tasks are the model update based on the process measurements (i.e., validation and adjustment of the model equations and parameter values) and gaining knowledge on the process (process know-how) with the help of the validated model. In case of generic models, e.g., model of circulated fluid bed combustor, the procedure is repeated when a new plant is constructed and new measurements become available. A typical evaluation test sequence (test matrix) available for modeling the combustion process is illustrated in Figure 2. In order to improve the model, the test sequence can be repeated. However, execution of dynamic tests in full scale plants is both expensive and time consuming. Therefore, efficient use of the existing measurement data for model validation is of primary interest, e.g., application of advanced optimization and/or search tools in the parameter estimation phase.

As discussed above already, imperfections in the model are only one of the potential reasons for mismatch between simulations and measurements. The mismatch can be due to measurement inaccuracies or unmeasured disturbances. Typical examples in the combustion processes include incorrect information on fuel characteristics (e.g., heat value, moisture, particle size distribution), or air flows (e.g., biased flow measurements, air leakages). A model which has been validated as highly reliable can support the evaluation of process measurement data.

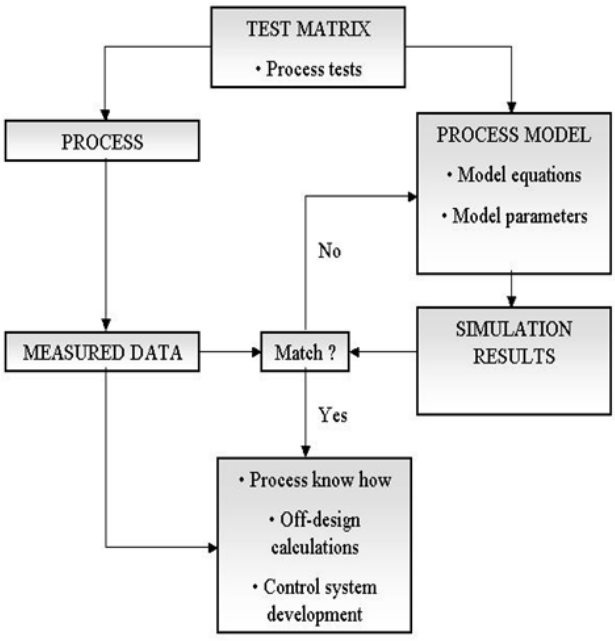

FIGURE 1. The procedure to develop a model and to generate process know-how

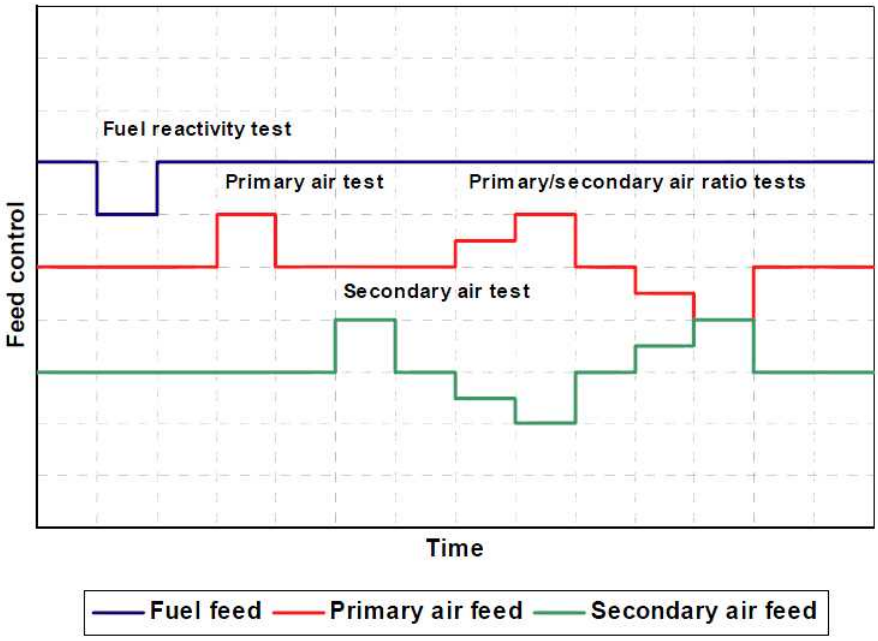

FIGURE 2. Dynamic tests [19]. Typical test series includes steps in fuel feed, primary air and secondary air. In addition, open and closed-loop load tests (steps/ramps) are commonly performed.

The main aim of the research reported in this paper was to examine the possibilities of developing an engineering tool for assessing the model vs. the measurements, and vice versa, in order to test and/or extract useful hypotheses during examination of dynamic test period outcomes. For example, the varying fuel moisture content or heat transfer coefficient can be considered, as the experimental sections show. The secondary goal of the work was to look at the potentials in combining large scale simulation models with modern state estimation techniques. A more accurate identification of process pathways will provide useful information for process design. In monitoring, a more realistic characterization of the plant state and/or parameters is valuable to process operators and engineers, up to enabling to build more advanced operating policies to be used in automatic control, for example.

Model calibration and state estimation. Parameter tuning considers finding the best values for a set of parameters, vs. given measurement data, under required parameter robustness, constraints, etc. Due to complexity of real life processes, simplifications often lead the model designer to fix time-varying parameters to constants. A typical time-varying behavior is due to a change in the operation point of a process, such as the load level or fuel mixture recipe in power plants. It is common to consider uniformly stirred reactors despite of channeling in real equipment, to simplify effects at phase boundaries, and many other approximations. The effective value of an originally physical variable or parameter then remains to be tuned using measurements, physical understanding, and backed up by engineering sense. Often the parameter uncertainty is as important a piece of knowledge as the actual value of the parameter itself, whether optimal or not.

This calibration of system parameters is often termed as parameter estimation. Parameter estimation is in itself an advanced field of science [13, 23, 31], particularly important in system identification and closely related with numerical optimization. Estimation of time-varying parameters is an essential part of adaptive control [33]. While rather efficient methods exist for parameter estimation in simple model structures (e.g., transfer

functions, linear regression models), the large dimensionality and nonlinearities associated with physical process models limit the applicability of many of the parameter estimation techniques common from system identification.

State estimation techniques can be applied to parameter estimation by incorporating the unknown parameter as (a part of) the unknown state, and looking at the problem as estimation of values of states with constant (time-invariant) true values. The Bayesian approach enables to combine a model with data records under the framework of stochastic systems. Given extended records of measurements it is possible to reason the values for past events and reduce the effect of process and measurement noise. In Bayesian dynamic models [2], the most natural option consists in treating the unknown parameter as a component of the state which has no dynamic evolution, and associating a stochastic (e.g., random walk-like) dynamic equation with a small variance with it. This straightforward approach was also considered in this work.

On-line state estimation refers to the task of estimating the plants current state vector (filtering), the state vector in the future (prediction), or the past states (smoothing), based on the measurement information up to (and often including) the current point in time. Since filtering alone will often yield only fairly uninformative (albeit up-to-date) state estimates, the look-ahead allowed by smoothing enables much more accurate estimates to be achieved retrospectively, and in many cases, highly specialized smoother algorithms can be developed [2]. This will be important when engineering evaluation is needed to judge the state estimates proposed by a numerical computational method, since typically the assessment is based on re-simulation of past data records and the on-line aspects are less important.

Engineering literature shows that the Bayesian approach is very efficient for solving this type of problems. The Kalman filter is a famous algorithm for the special case of linear models and Gaussian noise (innovations) [16]. The extended Kalman filter (EKF) relaxes the linearity assumption by considering locally linearized models. Particle filters (PF) were suggested first in 1993 for solving non-linear non-Gaussian problems [1, 4, 5, 9, 25, 26] and they are rapidly gaining ground also in industrial applications [2, 3, 14]. Other well known extensions of the basic Kalman filter include the unscented Kalman filter (UKF) and Rao-Blackwellized particle filter, just to name a few. A duality can be associated between the cost function in optimization and the distribution in the particle filtering (see [9, 25, 26]), similar to Kalman filtering, in the Bayesian sense.

Up-to-date, few applications of particle filtering have been reported in the area of power plant control and automation. Some relevant reports include applications for life cycle analysis (CO_2 emission analysis [32]); fault diagnosis (remaining useful life of steam generator tubes [20]); and nonlinear model-predictive control (MPC) using particle filtering-based state estimates (in oxy-fuel boiler control [6], or in a fluidized bed water softening application [30]), or particle-filtering-based optimization of control sequences (in a bubbling fluidized bed combustion [26]).

The reminder of the paper is organized as follows. The next section gives a brief overview to the circulating fluidized-bed (CFB) process and the hot-loop model used, followed by a description of the hot-loop parameter estimation (HOPE) problem. The initial studies on finding an optimal time-varying sequence for the unknown parameters are described in Section 4. Section 5 details the particle filtering approach to state estimation. Problem formulation, parameter set-up and simulation outcomes from a HOPE case study are reported in Section 6, including discussions on analysis of results and further extensions to on-line state estimation. Finally, concluding remarks and summary are provided in Section 7.

2. **The CFB Hot-Loop Model.** The hot-loop system is the heart of a circulating fluidized bed (CFB) power plant. This section gives a brief introduction to the CFB process, and to a dynamic model of the CFB furnace with solids recirculation, the hot-loop.

2.1. **The CFB process.** In a fluidized bed combustor, the fuel is combusted by mixing it with a large amount of inert material (sand or ash) fluidized by air (or by a mixture of recirculated flue gas and primary oxidant) [10]. In a CFB, see Figure 3, most of the inert material flows in a closed circle from furnace to cyclone and via the return leg back to furnace, forced by the primary gas blown from the bottom of the furnace. The inert material gives thermal stability, e.g., against disturbances in fuel properties, and the long residence time of the fuel in bed ensures complete combustion. Additional bubbling fluid bed heat exchanger INTREX^{TM} (by Foster Wheeler Energia Oy) installed at the bottom of the return leg, see Figure 4, improves further the heat balance of the furnace. The heat released during the combustion is transferred to water/steam via the furnace tubes (evaporator) and the heat transfer surfaces placed at the top of the furnace and in the flue gas path. Research on CFB has been active during the past decade, due to its flexibility to combust various multifuel mixtures with large variations in fuel quality, capabilities enabling combustion of biomass fuel fractions, and future extensions on oxy-fuel combustion on the basis of CFB technology [7]. Parallel, due to the need of high efficiency of electricity generation, boilers with super- and ultra supercritical steam generation cycles, i.e., the once-through boilers (OTU), are today in the focus. The combination of the CFB technology with OTU design is the front-runner solution in boiler technology; the first of such boilers was constructed in Lagisza power plant (460 MW_e, 45% plant efficiency with steam parameters 563°C/582°C and 282/51 bar) in 2009 [17].

The main operation of an industrial CFB includes the fuel and air flow supply. In order to ensure adequate combustion conditions (stoichiometry), the primary and secondary airs are distributed at several stages. The CFB operation needs to ensure security vs. carbon monoxide, good fluidization conditions, upper and lower bounds for bed and roof temperatures, and NO_x staging. Commonly, limestone is added to fuel to reduce SO_2 emissions. The effects of the main controlled and control variables are tightly coupled.

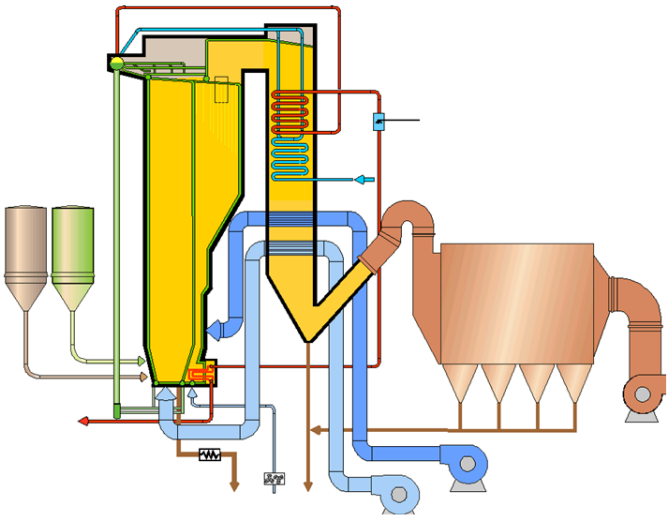

FIGURE 3. A once-through circulating fluidized bed boiler

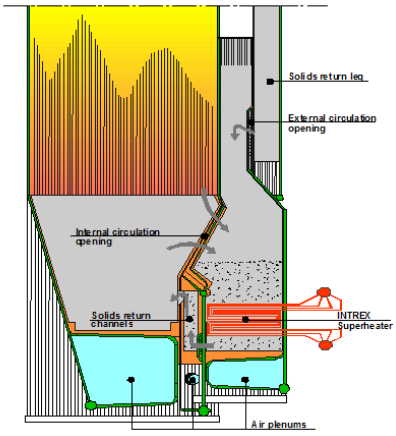

FIGURE 4. CFB furnace with an INTREX^{TM} construction

Many of the main characteristics of the process are impossible to measure on-line, including bed fuel inventory, bed inert mass, and particle size distribution in the furnace, or heat transfer coefficients in various parts of the boiler. They can be determined only vaguely or indirectly from the available measurements [11]. The main disturbances typically come from the varying fuel quality, where characteristics such as moisture, composition, (effective) heat value, fuel mix, and particle size distribution may be of interest. The sources of disturbances depend heavily on the type of fuel(s) used: coal, wood chips, peat, RDF, etc. The stability of the combustion and the bed has a high interest especially when the plant is operated at frequently varying load levels, due to large variations in the daily power demand or the participation of the unit in the electric grid frequency control. From maintenance point of view, avoidance of corrosion and unnecessary temperature stresses are important both in the furnace and at the heat transfer surfaces in later stages of the process.

Due to the complexity of the process, the reasoning of a human engineer examining the performance of the process can be greatly supported by an appropriate tool. The tool should be able to take into account the available quantified process knowledge (process models) and the expected sources of uncertainty (hypotheses) posed by the engineer. Such a tool was in the focus of the research reported in this paper.

2.2. **The CFB hot-loop model.** A hot-loop model has been developed at the Lappeenranta University of Technology (LUT) in cooperation with the Foster Wheeler Energia [8, 27] for static and dynamic simulation of CFB furnace phenomena. Separate submodels have been developed for different parts of the CFB loop, including furnace, solids separator, return channel and INTREX$^{\text{TM}}$. Each dynamic component model is based on the fundamental laws of conservation of mass, energy and momentum. In addition, empirical correlations have been built for fuel combustion, heat transfer and dynamics of circulating material. The model does not contain any steam side components, but it can be further connected to a water-steam simulator/process via heat transfer surfaces (heat exchangers). Their physical position can be exactly defined in the hot-loop model.

An overview of the hot-loop model is depicted in Figure 5. Simulation inputs include fuel and air feeds and their compositions, and heat surface temperatures, the input vector contains a few dozens of variables. The model consists of around 660 states, such as heat fluxes and temperatures and flue gas compositions, for the furnace, separator and INTREX$^{\text{TM}}$ subprocesses. Model outputs include the predicted flue gas concentrations, flows, and various temperatures, roughly one hundred variables in all.

The hot-loop model has been used for simulation of various pilot and full-scale CFB power plants [21, 27]. In particular, the performance of the model during load changes and its responses to individual control variables such as fuel, primary air and secondary air flow rates has been demonstrated for a number of commercial and pilot-sized plants. For the purpose of the current research, measurements of step and ramp experiments from two plants were available.

3. **The Hot-Loop Parameter Estimation (HOPE) Problem.** The original hot-loop system model (see Section 2.2) contains a large number of constant parameters. In the hot-loop parameter estimation (HOPE) problem, the assumption of constant valued parameters was relaxed for one or several parameters, $\boldsymbol{\theta}$. Given a set of selected parameters, the task was then to search for an unknown time varying vector $\boldsymbol{\theta}_k$, where k is the sampling instant, in order to make the model outputs match the measured outputs. In the validation phase, an engineer was assumed to judge, based on process knowledge and good

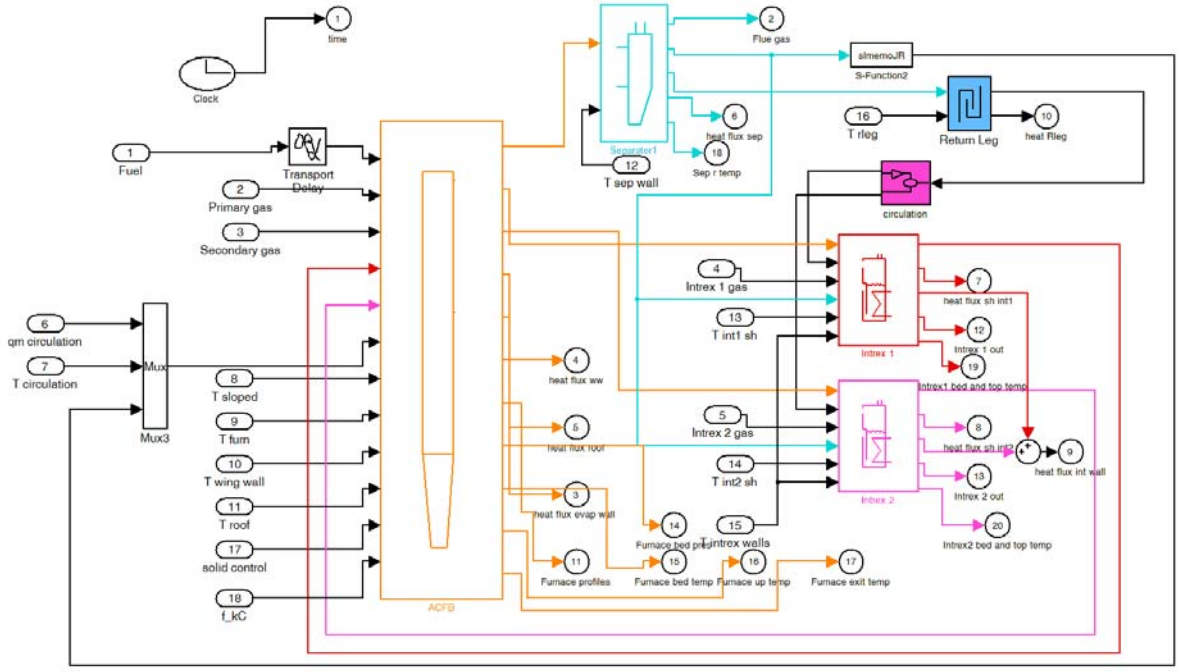

FIGURE 5. The hot-loop model consists of a riser, separator and two INTREX^{TM} units

engineering sense, whether these computed changes could explain the observed measurement records. The task of the HOPE project was to develop a tool which would help the engineer to evaluate and test various hypotheses, aiming at a good compromise between simulated and measured behavior, and leading to an improved understanding of the physical phenomena and plant behavior that took place during the test sequence.

In a particular case study, five time-varying variables were selected for a closer examination. The effective value for these parameters is uncertain, yet has a significant effect on combustion and heat transfer:

- char affinity, or burning rate coefficient (*fkc*),
- wing wall heat transfer coefficient (*fHTC1*),
- roof heat transfer coefficient (*fHTC2*),
- the furnace wall heat transfer coefficient (*fHTC3*), and
- fuel moisture coefficient (*fH2O*), i.e., the mass fraction of moisture in the fuel feed.

From simulation point of view, these five parameters were given as inputs to the hot-loop model, with nominal values normalized to ones. The study was based on experimental data from a full scale CFB. The main data set, the reactivity test data (see Figure 2), consisted of downwards and upwards steps in the fuel feed in open loop, a set of 301 measurements taken at a fixed sampling rate. Several other data sets were also available for examination.

The model behavior was optimized against selected cost functions. In this study, squared deviations between model and data in the flue gas O_2 concentration, c_{O_2}, and the furnace bed temperatures, T_B, were minimized,

$$J(\boldsymbol{\theta}) = ||c_{O_2} - \widehat{c}_{O_2}|| + ||T_B - \widehat{T}_B|| \tag{1}$$

as they reflect well the two important phenomena in the furnace: combustion and heat transfer. Also, relatively reliable measurements for these variables can be obtained from the process, both in pilot and commercial scale plants.

4. **Initial Studies.** In the first phase of the study, sensitivity of parameters was examined in simulations using time-invariant parameter values. For each of the five parameters, the value of the pth parameter at instant k, θ_k^p, was taken from a set $\{0.8, 0.9, 1, 1.1, 1.2\}$ of fixed values $\forall k$, while other parameters were set to nominal values, $\theta_k^q = 1$ for $q \neq p$. The whole reactivity test data set was then simulated with this parameter setting and the model outcomes compared with the measured ones to see which value gave the best output in terms of minimizing the cost function, Equation (1). Also the sensitivity of each of the five parameters vs. each of the outputs was examined based on these simulations with constant parameter values. The results were collected in a table of linearized static gains $\Delta y/\Delta\theta$ around nominal value of $\theta_k^p \equiv 1$. Table 1 shows the gains for four outputs (flue gas O_2 and three furnace temperatures) and the five parameters.

From these studies it was observed that the hot-loop temperatures were most sensitive to the third heat transfer coefficient (*fHTC3*), and that the fuel moisture content (*fH2O*) had the strongest effect on the flue gas O_2 concentration. *fH2O* had a positive gain on flue gas O_2 and negative gain on furnace temperature. For the other parameters, the gains were small up to having practically no effect on any of the outputs. In particular, the burning rate coefficient (*fkc*) had only transient significance, albeit the transient responses could be strong.

4.1. **Batch optimization.** The study with constant values was followed by a simultaneous optimization of sets of either one, three, or all five parameters. The sequence of selected parameters was optimized using a gradient-based search algorithm. The cost function to be minimized consisted of a sum of squared errors on either the oxygen concentration, or both O_2 and furnace bed temperature, as in Equation (1). In the case of two terms in the cost function the errors were scaled so that roughly a 50% balance between both terms was obtained.

In the gradient-based approach the sample-gradients were evaluated by making small random disturbances to parameter values around the current best solution and re-simulating. Consequently, a large number of parameters in a sequence would consume a lot of computing power. Therefore, the number of estimated parameters was reduced by using time intervals, during which the parameter value was considered either constant (zero-order hold), or linearly interpolated (first order hold). The assumption on the smoothness of parameter changes is also supported by physical arguments.

With the given data set and 16 parameter intervals, 17 simulations at each iteration were required. As a typical number of iterations required for convergence was around a few tens, the approach required a few hundreds of simulations of the test sequence for each examined set of parameters. Consequently, the simulations were quite time consuming, and were performed overnight or over weekends.

TABLE 1. Static gains. Rows: parameter θ^p, columns: output y^o (the gain $\Delta y^o/\Delta\theta^p$ around the nominal value $\boldsymbol{\theta} = \mathbf{1}$).

	O_2	T_{bed}	T_{roof}	T_{exit}
fkc	–0.001	–0.268	–0.198	–0.197
$fHTC1$	0	–34.158	–40.778	–44.006
$fHTC2$	0	–2.885	–5.744	–4.760
$fHTC3$	0	–117.020	–131.180	–135.530
$fH2O$	2.459	–64.161	–60.625	–58.721

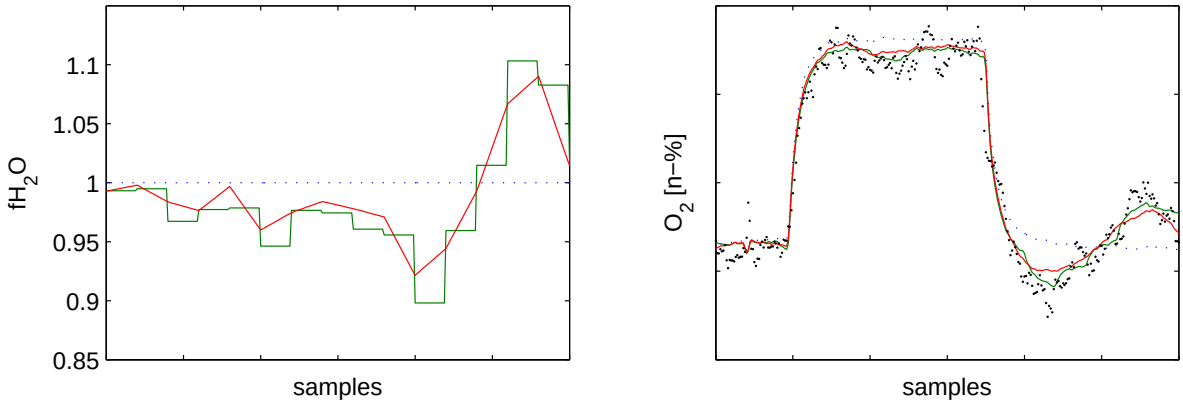

FIGURE 6. Simulation outcomes using zero and first order interpolation between optimized parameter values (intervals). The dotted lines show the response with a constant $\boldsymbol{\theta}_k \equiv \mathbf{1}$.

A typical simulation outcome is illustrated in Figure 6 where the examined parameter is *fH2O*. The figure shows the measured flue gas oxygen, and outcomes from three simulations: using a constant value $\theta = 1$, using optimized values with a 0-order hold, and optimized values with a first-order hold. The variables are shown in normalized scales due to data confidentiality reasons. With the chosen interval length and a 0-order hold, the optimization approach resulted in step-like changes in the parameter values about every 30 samples. Using interpolated changes, the slope of the parameter value curve changed at every 30 samples, passing through the points determined in the optimization.

From Figure 6, it is clear that a time-varying moisture content explains much better the oxygen data, compared with using a constant value. The changes in moisture content seem feasible ($\pm 10\%$ around nominal value during the simulation), and were further confirmed by the responses in temperatures (not shown here). The impact of *fkc* transients was particularly well seen in optimization studies using 0-order hold, and the transients dominated the response (not shown here). Therefore, the step approach was omitted from further simulations, and only the interpolated parameter changes were considered in the sequel.

4.2. **Motivation for further research.** It seems clear from the initial studies that the basic approach of the HOPE is valid. The assumption of a fixed parameter value was relaxed to a time-varying value for a selected set of parameters (i.e., hypotheses). The HOPE-approach generated (via optimization) a scenario which better explains the observed data. The outcomes are then to be further evaluated by the research engineer who is able to process them in the larger context of all related information, e.g., experiment test circumstances, validity of the model, and condition of the measurements.

However, in order to provide a useful tool for the engineer in the support of hypothesis testing, the computation times can not be excessive, and should be measured in minutes if not in seconds. It would also be useful if information concerning the uncertainties involved with various scenarios would be clearly conveyed to the end-user. With the fixed step-size gradient-based approach, the evaluation of gradients may become a limiting factor in terms of required time and computer power, when the number of parameters is large. Problems were also observed with the stability and robustness of the search with sample gradient evaluation. Significant reductions in the simulation times can be achieved by noting that all intervals do not need to be re-simulated at all times. Quite obviously, it would also be advisable to examine more advanced gradient-based optimization algorithms if this line

of approach was to be pursued further. More efficient algorithms may also be found by examination of (heuristic) random search approaches, which perform a direct search with no need to evaluate sample gradients. Yet another option would be to develop further the idea of parameterization of the time-dependence of the θ's. In this work, however, algorithms based on sequential state estimation were explored, due to the attractiveness of the Bayesian formulation in terms of the speed of computations (sequentiality) and the possibility to take uncertainties into account (probability distributions).

5. **State Estimation.** An alternative view to approach the issue of model calibration is to cast it as a state estimation problem. In this case, we consider parameters $\boldsymbol{\theta}_k$ to belong to the system state vector $\mathbf{x}_k$, and attempt to reason the proper value of the state based on a model of the system and measurements from it. The well-known solutions for linear or close-to-linear systems are the Kalman filter and the extended Kalman filter. For non-linear systems, the unscented Kalman filter and the particle filter are the two leading candidates proposed in the literature [22]. Unlike the Kalman filter, the particle filtering approach is not limited by the linear-Gaussian assumptions, and particle filtering algorithms can handle complex dynamics, such as discrete jumps, or multi-modal densities. However, the approach may be computationally intensive, and the advent of cheap powerful computers has been the key to the success of particle filters.

5.1. **Sequential search with particle filters.** Monte Carlo methods are computational algorithms that rely on repeated random sampling to compute their results. A particle filter (PF) [28] is a sequential Monte Carlo implementation of the Bayesian filter. Instead of describing the required probability density function (pdf) in a functional form, the pdf is represented approximately by a set of random samples from the pdf. The approximation can be made as good as necessary by choosing the number of samples N; as $N \to \infty$, the approximation becomes an exact equivalent of the functional form. These random samples are the 'particles' of the particle filter. They are propagated and updated according to the models for system dynamics and measurements in a PF algorithm.

A dynamic model describes how the state vector evolves with time, a measurement equation relates the received measurement to the state vector:

$$\mathbf{x}_{k+1} = f_k(\mathbf{x}_k, \mathbf{w}_k) \tag{2}$$

$$\mathbf{y}_k = h_k(\mathbf{x}_k, \mathbf{v}_k) \tag{3}$$

where

- k is the sampling instant ($t = kT$, where T is the sampling interval and t is the real time);
- $\mathbf{x}$ is the state vector to be estimated, the pdf of $\mathbf{x}_0$ is assumed to be known;
- f and h are known (possibly non-linear) functions;
- $\mathbf{w}$ is a white noise sequence (the process noise), the pdf of $\mathbf{w}$ is assumed to be known;
- $\mathbf{y}$ is the vector of received measurements;
- $\mathbf{v}$ is a white noise sequence (the measurement noise), the pdf of $\mathbf{v}$ is assumed to be known and independent of $\mathbf{w}$.

Equation (2) defines a Markov process. An equivalent probabilistic description of the state evolution is $p(\mathbf{x}_{k+1}|\mathbf{x}_k)$, the transition density. An equivalent probabilistic model for (3) is $p(\mathbf{y}_k|\mathbf{x}_k)$. With initial conditions $p(\mathbf{x}_0)$ the specification is complete.

In the Bayesian approach, one attempts to construct the posterior pdf of the state vector: $p(\mathbf{x}_k|\mathbf{Y}_k)$, where $\mathbf{Y}_k$ denotes the set of all measurements received up to and including instant k, $\mathbf{Y}_k = \{\mathbf{y}_1, \mathbf{y}_2, \ldots, \mathbf{y}_k\}$. The initial condition is given by $p(\mathbf{x}_0|\mathbf{Y}_0)$ where $\mathbf{Y}_0$ is the empty set. The formal Bayesian filter consists of prediction and update

operations. The prediction operation propagates the posterior pdf at instant $k-1$ to a prior at k:

$$\underbrace{p\left(\mathbf{x}_k|\mathbf{Y}_{k-1}\right)}_{\text{prior at } k} = \int \underbrace{p\left(\mathbf{x}_k|\mathbf{x}_{k-1}\right)}_{\text{dynamics}} \underbrace{p\left(\mathbf{x}_{k-1}|\mathbf{Y}_{k-1}\right)}_{\text{posterior from } k-1} d\mathbf{x}_{k-1}$$

The prior pdf may be updated with the new measurement $\mathbf{y}_k$:

$$\underbrace{p\left(\mathbf{x}_k|\mathbf{Y}_k\right)}_{\text{posterior}} = \underbrace{p\left(\mathbf{y}_k|\mathbf{x}_k\right)}_{\text{likelihood}} \underbrace{p\left(\mathbf{x}_k|\mathbf{Y}_{k-1}\right)}_{\text{prior}} \Big/ \underbrace{p\left(\mathbf{y}_k|\mathbf{Y}_{k-1}\right)}_{\text{normalization}}$$

where $p\left(\mathbf{y}_k|\mathbf{Y}_{k-1}\right) = \int p\left(\mathbf{y}_k|\mathbf{x}_k\right) p\left(\mathbf{x}_k|\mathbf{Y}_{k-1}\right) d\mathbf{x}_k$. The measurement likelihood $p\left(\mathbf{y}_k|\mathbf{x}_k\right)$ is regarded as a function of $\mathbf{x}$ given $\mathbf{y}$. In the linear-Gaussian case, an exact closed-form solution to the Bayesian state estimation problem exists: the Kalman filter. With linearization, the approach can be extended to mildly non-linear processes (EKF). For grossly non-linear problems, the particle filtering provides an approximate solution. One of the most commonly used PF algorithms is the sampling importance resampling algorithm.

5.2. **Sampling importance resampling (SIR).** This basic particle filtering algorithm can be seen as a direct mechanization of the formal Bayesian filter [28]:

1. Suppose that a set of N random samples from the posterior pdf $p\left(\mathbf{x}_{k-1}|\mathbf{Y}_{k-1}\right)$ are available. Denote these particles by
$$\left\{\mathbf{x}_{k-1}^i\right\}_{i=1}^N$$
i.e., a set of N particles indexed by i from 1 to N.
2. The *prediction* phase consists of passing each of these posterior particles (from instant $k-1$) through the system model (2) to generate a set of prior particles (at k)
$$\overline{\mathbf{x}}_k^i = f_k\left(\mathbf{x}_{k-1}^i, \mathbf{w}_{k-1}^i\right)$$
where $\mathbf{w}_{k-1}^i$ is an independent sample drawn from the pdf of the process noise. This procedure produces a set of particles from the prior pdf $p\left(\mathbf{x}_k|\mathbf{Y}_{k-1}\right)$.
3. The *update* phase consists of calculation of a weight for each particle, normalization of the weights, and resampling according to the normalized weights. A weight $\overline{\omega}_k^i$ is calculated for each particle, based on the measurement likelihood (density function) evaluated at the value of the prior sample (and measurement):
$$\overline{\omega}_k^i = p\left(\mathbf{y}_k|\overline{\mathbf{x}}_k^i\right). \tag{4}$$
The weights are then normalized so that they sum to unity: $\omega_k^i = \frac{\overline{\omega}_k^i}{\sum_{j=1}^N \overline{\omega}_k^j}$. The prior particles are resampled (with replacement) according to the normalized weights to produce a new set of particles
$$\left\{\mathbf{x}_k^i\right\}_{i=1}^N \text{ such that } \Pr\left\{\mathbf{x}_k^i = \overline{\mathbf{x}}_k^j\right\} = \omega_k^j \text{ for all } j \text{ and } i$$
In other words, a member of the set of prior particles is chosen with a probability equal to its normalized weight, and this procedure is repeated N times to build up a new set of posterior particles.
4. The new set of particles
$$\left\{\mathbf{x}_k^i\right\}_{i=1}^N$$
are samples of the posterior pdf at k, $p\left(\mathbf{x}_k|\mathbf{Y}_k\right)$. The cycle of the algorithm is complete, and we continue from Step 2.

As with the Kalman filtering algorithm, we can add a deterministic system input $\mathbf{u}_{k-1}$ (plant control manipulations) to Step 2:

$$\overline{\mathbf{x}}_k^i = f_k\left(\mathbf{x}_{k-1}^i, \mathbf{u}_{k-1}, \mathbf{w}_{k-1}^i\right).$$

The rest of the algorithm remains intact.

The measurement likelihood (4) can be interpreted as an indicator of those regions of the state-space that are plausible explanations of the observed measurement value [28]:

- If the value of the likelihood function is high, these state values are well supported by the measurement.
- If the likelihood is low, these state values are unlikely.
- If the likelihood is zero, these state values are incompatible with the measurement model.

This simple algorithm [5] is today known as the Sampling Importance Resampling (SIR) filter. A long list of more advanced particle filtering algorithms have been and are being developed (see, e.g., overviews [1, 2]), based on a wise choice of the sampling importance; a fusion with Kalman filtering, unscented transforms, etc. For the purposes of the hot-loop analysis and tuning, examination of various PF algorithms was not in the main focus. Instead, particle filters were examined as a means to perform simulation-based sequential optimization for (potentially) non-linear/non-Gaussian models/uncertainties. Therefore, the widely used SIR algorithm was used also in the simulations in this study.

5.3. **Unscented Kalman filter.** A significant practical problem with the particle filters is the excessive computational load associated with the simulations. The number of required particles may easily increase, such that the needs for computational power would require investments to computational facilities beyond economically reasonable limits. If particle filters are then applied with insufficient computational resources, the long simulation times make the approach infeasible for practical engineering purposes. Therefore, a large amount of effort in particle filtering research is currently devoted to finding computationally efficient algorithms [29].

Alternatively, the assumptions on the underlying process can be tightened, which then justifies the application of more restricted but computationally less demanding algorithms. The Kalman filter of course is an example of such an approach, making assumptions of linearity and normality. Extended Kalman filters (EKF) relax the assumption of linearity into locally linearizable systems. The unscented Kalman filters (UKF) make the assumption that the distribution can be adequately described by its mean and covariance, only. Hence, e.g., potentially bimodal distributions should not be considered.

The UKF uses a deterministic sampling technique to pick a minimal set of sample points: the sigma points. These samples, situated around the mean, are then propagated through the nonlinear plant function, and the mean and the covariance of the estimate are recovered. Compared with particle filters the number of sigma points (cf. particles in particle filtering) is small. The advantage over EKF is that there is no need to explicitly evaluate the Jacobians.

The outline of the UKF algorithm is as follows, for details see [18, 24]:

1. Generate sigma-points, $\mathcal{X}_{k-1}^a$, such that they have a given sample mean and covariance, $\hat{\mathbf{x}}_{k-1|k-1}$ and $\mathbf{P}_{k-1|k-1}$.
2. Propagate each point through the process model f_k, $\mathcal{X}_{k|k-1}^a$.
3. Estimate the prior mean and covariance, $\hat{\mathbf{x}}_{k|k-1}$ and $\mathbf{P}_{k|k-1}$, by taking a weighted average.
4. Propagate each prior point through the measurement model h_k, $\mathcal{Y}_{k|k-1}$.
5. Predict the output, $\hat{\mathbf{y}}_{k|k-1}$, by taking a weighted average.

6. Compute the innovation covariance, $\mathbf{P}_{yy}$, and the cross correlation matrix, $\mathbf{P}_{xy}$. Compute the gain, $\mathbf{K}_k = \mathbf{P}_{xy}\mathbf{P}_{yy}^{-1}$.
7. Estimate the posterior mean and covariance,

$$\hat{\mathbf{x}}_{k|k} = \hat{\mathbf{x}}_{k|k-1} + \mathbf{K}_k(\mathbf{y}_k - \hat{\mathbf{y}}_k)$$

$$\mathbf{P}_{k|k} = \mathbf{P}_{k|k-1} - \mathbf{K}_k\mathbf{P}_{yy}\mathbf{K}_k^T.$$

8. Increase the sample counter k and return to generation of sigma points.

In this paper, the UKF is used to compare/validate the results obtained using SIR particle filters in the section concerned with on-line filtering (Section 6.5).

6. **Simulations.** This section reports numerical results from a specific case study of the HOPE problem. The detailed algorithm is first given, followed by presentation and analysis of the computer simulations based on data from a full scale power plant.

6.1. **Hot-loop model in state-space form.** For the purposes of parameter estimation, the hot-loop model (cf. Figure 5) first needed to be converted into a discrete-time state-space form assumed by the particle filter:

$$\mathbf{x}_{k+1} = f(\mathbf{x}_k, \mathbf{u}_k, \mathbf{w}_k) \tag{5}$$

$$\mathbf{y}_k = h(\mathbf{x}_k, \mathbf{v}_k) \tag{6}$$

Whereas, we always know that any simulation model can be converted into such a form, the practical implementation can be tedious. In our case, a simplification was made in that separate evaluation of f and h was considered unnecessary, i.e., we always evaluated the next state and together with the corresponding measurements. This assumption is valid for the SIR algorithm.

The hot-loop model state vector, $\mathbf{x}^{\mathrm{h}}$, consists of 660 states (see Section 2.2). In the state-estimation approach the state is now extended with the unknown parameter vector $\boldsymbol{\theta}_k$. It was considered that the parameters evolve as constants (i.e., random walk). The control inputs to the hot-loop model, $\mathbf{u}_k$, were read from the plant measurement data file. Due to the first-order nature in the interpretation of model inputs, also the past 20 control actions $\mathbf{u}_{k-1}$ were included in the state. Putting the building blocks together, the system model f is a time-invariant function with a state vector $\mathbf{x}_k$, the state $\mathbf{x}_k$ consisting of the original hot-loop model states $\mathbf{x}^{\mathrm{h}}$, a vector storing the past control manipulations $\mathbf{x}_k^{\mathrm{u}} = \mathbf{u}_{k-1}$, and a random walk term for each unknown parameter in $\boldsymbol{\theta}$:

$$x_{k+1}^{\mathrm{p}} = x_k^{\mathrm{p}} + w_k^{\mathrm{p}}$$

where w_k^{p} are the elements of $\mathbf{w}_k$, the state noise (a tunable parameter vector). The noises w_k^p are drawn from a known distribution, during simulations we need to provide realizations for them. In all, the size of the PF state estimation problem state vector is $|\mathbf{x}| = \left|\mathbf{x}^{\mathrm{h}}\right| + |\mathbf{x}^{\mathrm{u}}| + |\theta| = 685$.

The measurement model h is a time-invariant function within the hot-loop model, producing the 108 outputs. From optimization point of view, the essential measurements are the flue gas O_2 and furnace bed temperature. For these output variables we need to be able to evaluate the density $p\left(\mathbf{y}_k|\overline{\mathbf{x}}_k^i\right)$, i.e., the probability that a state vector $\overline{\mathbf{x}}_k^i$ results in a measurement vector $\mathbf{y}_k$. As a basic assumption, we consider the outputs to be distributed around the hot-loop model outcomes:

$$\mathbf{y}_k = \mathbf{y}_k^{\mathrm{h}} + \mathbf{v}_k,$$

where $\mathbf{v}_k$ are a from a known distribution (a tunable parameter reflecting the noise in the measurements).

6.2. **Algorithm and simulation set-up.** A pseudo-code for the parameter estimation procedure is shown in Algorithm 1.

Algorithm 1 HOPE PF algorithm

Initialize algorithm parameters (N, $\mathbf{\Sigma_x}$, $\mathbf{\Sigma_y}$) and particle states $\mathbf{x}_0^i$. ▷ prior knowledge
for k=1...K **do** ▷ for each sample
  Read measurement data: $\mathbf{u}_k$ and $\mathbf{y}_{k+1}$.
  for $i = 1...N$ **do** ▷ for each particle
    Read particle state $\mathbf{x}_k^i$ and extract $\mathbf{x}_k^{\mathrm{h},i}$, $\mathbf{u}_{k-1}$ and $\boldsymbol{\theta}_{k-1}^i$.
    Generate $\mathbf{w}_k^i \sim \mathcal{N}(\mathbf{0}, \mathbf{\Sigma_x})$. ▷ exploration
    Compute $\boldsymbol{\theta}_k^i = \boldsymbol{\theta}_{k-1}^i + \mathbf{w}_k^i$.
    Ensure parameter bounds $\boldsymbol{\theta}_{\min} \leq \boldsymbol{\theta}_k^i \leq \boldsymbol{\theta}_{\max}$.
    Simulate hot-loop model $\mathbf{x}_{k+1}^{\mathrm{h},i} = f(\mathbf{x}_k^{\mathrm{h},i}, \mathbf{u}_k, \mathbf{u}_{k-1}, \boldsymbol{\theta}_k^i, \boldsymbol{\theta}_{k-1}^i)$. ▷ simulation[1]
    Append and store particle state $\mathbf{x}_{k+1}^i$.
    Simulate hot-loop model measurement equations $\mathbf{y}_{k+1}^{\mathrm{h}} = h(\mathbf{x}_{k+1}^{\mathrm{h},i})$.
    Weigh particle by evaluating $\overline{\omega}_{k+1}^i = \mathcal{N}(\mathbf{y}_{k+1} - \mathbf{y}_{k+1}^{\mathrm{h}}, \mathbf{\Sigma_y})$. ▷ measurement
  end for
  Normalize particle weights ω_{k+1}^i.
  Resample particle population with replacement. ▷ SIR
  Compute on-line statistics of interest. ▷ application
end for
Compute statistics of interest. ▷ application

In the algorithm set-up the distributions for $\mathbf{w}_k$ and $\mathbf{v}_k$ need to be fixed, as well as the number of particles N. Based on the initial studies (Section 4), two parameters were considered to be sufficient for the simulations: the fuel moisture *fH2O* and the furnace wall heat transfer coefficient *fHTC3*. For simplicity, both w's and v's were drawn from normal distribution (note that this assumption is not required by the algorithm):

$$w_k^p \sim \mathcal{N}\left(0, \sigma_p^2\right), \quad v_k^m \sim \mathcal{N}\left(0, \sigma_m^2\right)$$

where p and m are the indexes running through all parameters under examination and all outputs in the cost function. In the current setting, $p = 1, 2$ and $m = 1, 2$. A standard deviation of $\sigma_p = 0.01$ was used for the parameters. In addition, upper and lower hard constraints were set on the parameters in $\boldsymbol{\theta}_k$

$$\frac{1}{2} < \theta_k^p < 2$$

(recall that the nominal value for each parameter was 1). For the O_2, a standard deviation of 0.2%-units was used, for bed temperatures a standard deviation was set to 5°C. A few test simulations in the vicinity of these values were carried out to ensure a proper balance between exploration, state smoothness, and ability to follow the measurements. The stochastic exploration in the search is tuned using the parameters of the density characterizing $\mathbf{w}_k$. This should reflect the expected variability of the corresponding physical phenomena, as well as the uncertainty in the initial values. In practice, a few simulations were required to tune these parameters for an adequate response.

A large population size N is desired in order to have an accurate sample representation of the state pdf; on the other hand, the simulation times become excessive with N. In the case study, the size of the particle population was largely determined by the hot-loop

[1]Hot-loop model simulation uses 1st order interpolated inputs.

model software. The software was written and compiled so that it had to be executed in a 32-bit Windows environment, which restricted the population sizes to max 2000 particles. $N = 500$ was used in the numerical results reported here.

The data for the simulations was taken from a reactivity test conducted for a full scale power plant, a set of 301 data sample rows. Due to confidentiality reasons, the numerical values for time and variables/parameters can only be published in a linearly normalized scale (denoted by n-% in the figures). The 'normal operation' scale for the variable was in the range of 0-100%. The initial state for the hot-loop model was taken as the steady state calculated using the first measured control vector, and using $\theta_0^1 = 0.95$ (for *fH2O*) and $\theta_0^2 = 1.5$ (for *fHTC3*), based on initial studies (see Section 4). A mex-compiled furnace model (version 2.26) was run in Simulink, by the particle filtering algorithm implemented in Matlab. The simulations were run in Matlab 7 2010b on a standard office PC with a 3GHz i7 CPU.

6.3. **Simulation runs.** Recall Figure 6, which shows the flue gas oxygen response for a hot-loop model with constant parameters (i.e., nominal case $\boldsymbol{\theta}_k \equiv \mathbf{1}$, dotted line), as well as the interval-based time-varying estimates from initial studies. Figures 7-10 illustrate the corresponding simulations with the PF approach. The smoothing estimates $\widehat{\mathbf{x}}_{k|K}$ are considered first; the filtering estimates $\widehat{\mathbf{x}}_{k|k}$ are discussed in Section 6.5.

The figures show the quantiles of the variable distributions, as approximated by the population of $N = 500$ particles. The figures show the 1% and 99% quantiles (light gray), 20% and 80% quantiles (medium gray), and the 50% quantile (black). In addition, three randomly chosen sequences among the population are plotted (by thin red, blue and green lines). When appropriate, the corresponding measurements are shown by dots, as in Figures 7 and 8. Figure 7 depicts the flue gas O_2 concentration, c_{O_2}, during the test sequence; Figure 8 shows the furnace bed temperature, T_B. The simulated O_2 and T_B follow the measurements well. The estimated parameters and their distributions for the fuel moisture and heat transfer coefficient are illustrated in Figures 9 and 10, respectively. For the fuel moisture parameter, behavior similar to that observed already in Figure 6 can

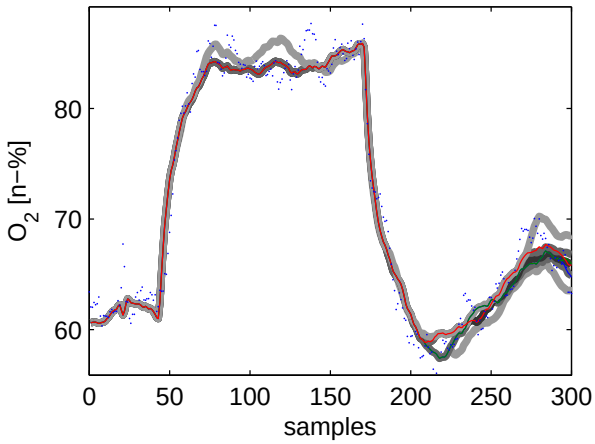

FIGURE 7. Measured (dots) and estimated (solid lines) flue gas oxygen concentrations. The quantiles of the estimated distribution are shown in gray scale.

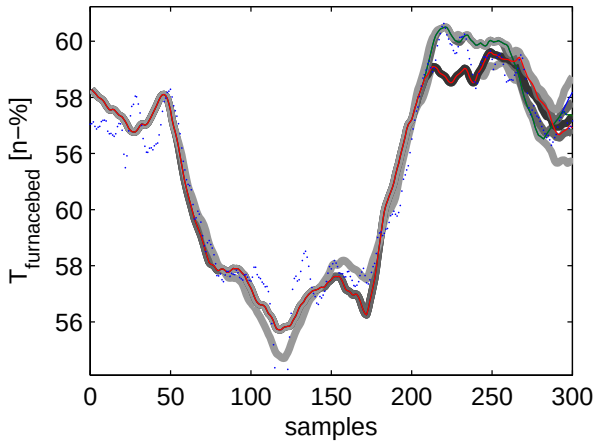

FIGURE 8. Measured (dots) and estimated (solid lines) furnace bed temperatures

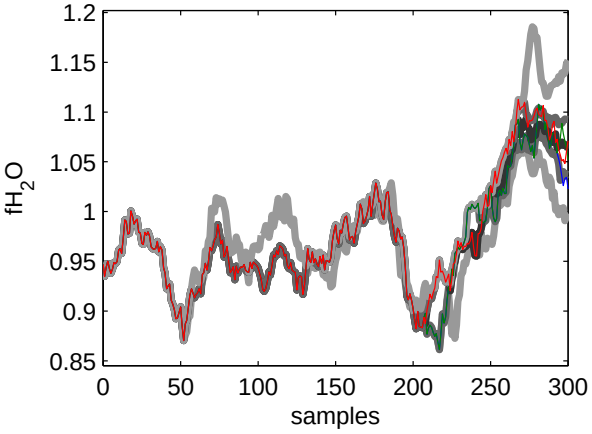

FIGURE 9. Estimated fuel moisture correction coefficients ($fH2O_{k|K}$)

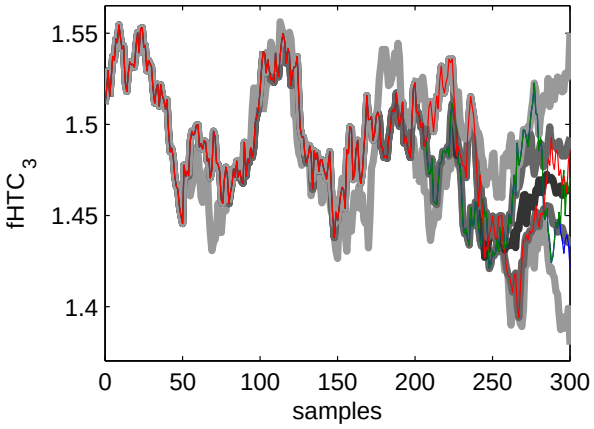

FIGURE 10. Estimated heat transfer correction coefficients ($fHTC_{k|K}$)

be noticed. The estimate for the heat transfer coefficient remains in the neighborhood of the fixed value 1.5, which is also in accordance to initial studies.

Uncertainties associated with the parameter estimates become visible by examination of the population quantiles. For smoother estimates, it is natural that the uncertainty increases as the end of the data record is approached, as the length of the look-ahead window decreases. This is clearly visible in the plots for the parameter estimates, and in the associated simulations of the outputs c_{O_2} and T_B. In fact, the PF population for the first 50 samples appears to have converged into a single copy. For the estimates close to the end of the data set, the distribution approaches that of a filter (Section 6.5). Figure 11 shows the sample estimate of the efficient sample size, $\widehat{N}^{\text{sample}}_{\text{eff,k|K}}$ (see [12]). Cutting corners, this indicates the number of different particles in the population at instant K that describe the estimated pdf at sample k. Indeed, it appears that before the first step (decrease in fuel, increase in O_2) the population contains only one trajectory. After the second step (increase in fuel, decrease in O_2) the number of different particles increases quickly, up to N at the end of the simulation.

The execution time for a particle filter-based simulation was measured rather in hours than in minutes, most of the computations (over 95% of computing time) were spent in the $KN = 150000$ one-step-ahead simulations of the hot-loop model.

6.4. **Analysis.** Figure 9 shows the estimated parameter *fH2O*. Comparing Figure 7 with Figure 6 using a constant-valued *fH2O* it is clear that the on-line adjustment of the fuel moisture content is indeed a parameter which strongly effects the behavior of the combustion process. The figure suggests that that a more appropriate value for the fuel moisture content coefficient is below the nominal 1, and the uncertainty analysis further supports this finding. However, at the end of simulations an upward trend in the fuel moisture would explain well the peculiarities in the flue gas O_2 content. This is also confirmed by the good fit in the temperatures, such as the furnace bed temperature shown in Figure 8. Hence, the hypothesis of a time-varying moisture content appears to be supported by the particle filter estimate, i.e., the model and the data. It is justified to make the conclusion that indeed the input information concerning (a constant) moisture content should be relaxed, and that it is quite possible that the moisture content changed towards the end of the experiment.

Figure 10 shows the estimated parameter *fHTC3*. The heat transfer coefficient value remains at a fixed level around $1.4 - 1.5$, and the model is able to follow the main trends in the temperatures. Many of the smaller peaks down- and upwards (see Figure 8) cannot be well explained by the model, and the state estimator neglects much of these peaks in the temperatures. The value of the parameter stays within a relatively narrow area, and the analysis seems to indicate that the heat transfer coefficient is a constant coefficient. However, a further modeling effort might be justified, such as creating a model $\theta = g(\mathbf{x})$ for the *fHTC3*, based, e.g., on furnace velocities.

While the finding itself may not be surprising, it is important to be able to systematically detect and quantify the changes in the parameters that explain the observed behavior, and the uncertainties involved in the estimation. This is the major function of the tool that was looked for in the HOPE project.

6.5. **On-line state estimation.** In addition to analysis and tuning of existing models and their signals, once designed, the approach also proposes a possible filter to be used for on-line state estimation.

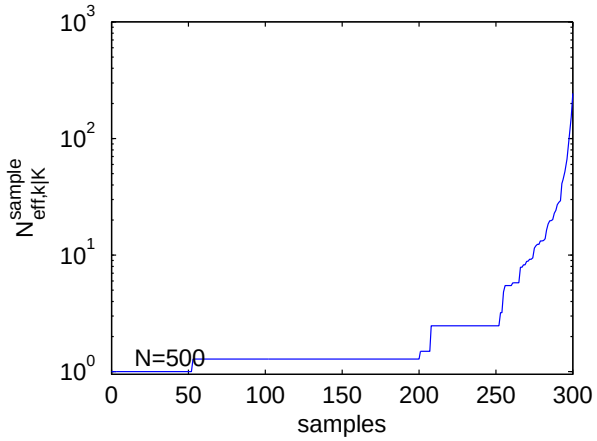

FIGURE 11. Sample estimate of the efficient sample size

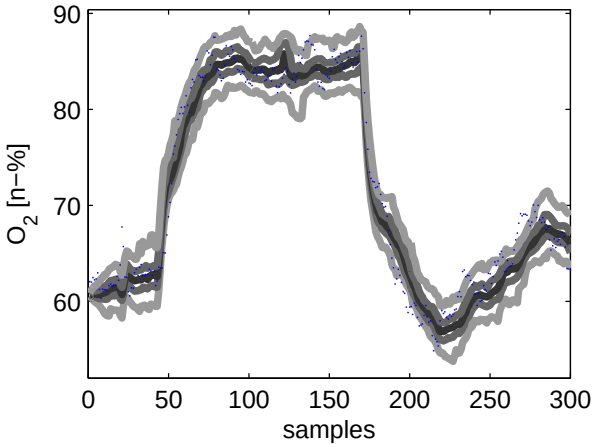

FIGURE 12. Measured (dots) and estimated (solid lines) flue gas oxygen concentrations

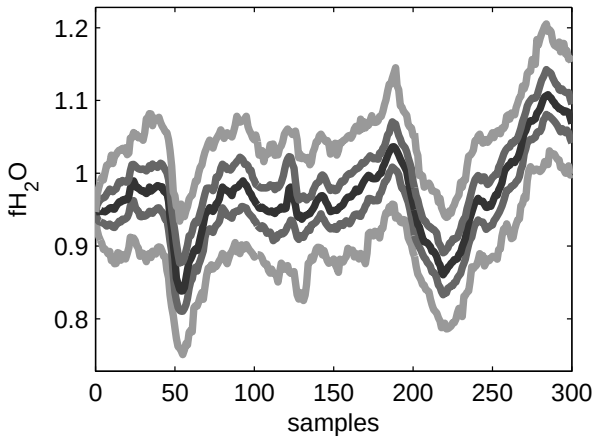

FIGURE 13. Estimated fuel moisture correction coefficients ($fH2O_{k|k}$)

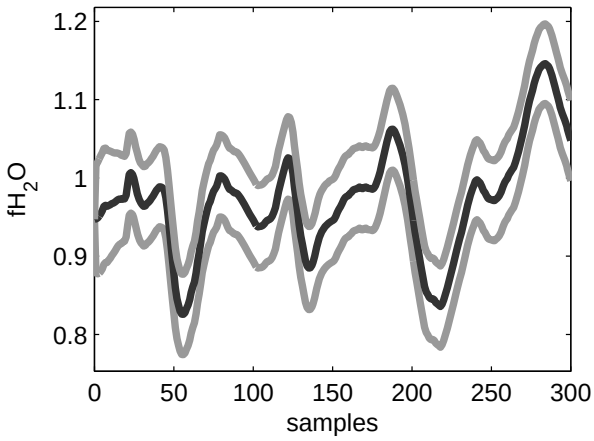

FIGURE 14. Fuel moisture correction coefficients ($fH2O_{k|k}$) estimated using UKF

Figures 12 and 13 illustrate filter estimates for the samples in the data set, i.e., estimates computed based on the information up to (but not exceeding) instant k. Hence, this type of estimates can be computed on-line already. The uncertainty in the on-line estimates $(k|k)$ is substantially larger compared to smoothed estimates $(k|K)$. This is the more true, the closer to the beginning of the test sequence we move to. However, useful information can still be extracted from the filter distributions, too. During the first half of the sequence, there is a relatively high certainty that the moisture coefficient at 1 is overestimated (see Figure 13), also the increase at the end of the sequence is visible on-line already.

Figure 14 shows the corresponding outcome using the UKF, illustrating the mean and 2×standard deviations for the fuel moisture parameter. The similarity of the estimated distribution with that obtained using particle filtering is obvious (see Figure 13). The computational load is highly decreased with the UKF, as only 5 sigma points need to be evaluated, compared with the $N = 500$ in the PF simulations. However, in general, the validity of the UKF assumptions depends on the problem at hand.

The on-line information is extremely valuable for monitoring and control purposes, as proper knowledge of system state and its uncertainty enables to assess the plant state and to find the correct feedback actions that need to be taken. However, the use of such information is not straightforward. Typically, only the expected state value is used for feedback control (see., e.g., [30]), and it is not easy to illustrate efficiently the uncertainties associated with the process variables to the process operators either. The currently available methods, such as finite state optimal control [9] have only been demonstrated in small scale problems. Clearly, more research is required to find methods which take full advantage of the increased information, as well as means to assess whether the improved monitoring/control justifies the investments required, e.g., for improved computational power.

7. **Discussion and Conclusions.** This work proposed an approach based on Bayesian reasoning under the particle filtering paradigm, to be used for analysis of experimental test sequences from full scale industrial processes, with the help of a first-principle-based process model. The assumption of a fixed parameter value was relaxed to a time-varying value for a selected set of parameters. The HOPE-approach generated (via optimization) a scenario which better explains the observed data. The outcomes are then to be further evaluated by a research engineer, who is able to process them in the larger context of all related information, e.g., experiment test circumstances, validity of the model, and condition of the measurements.

An algorithm based on sequential state estimation was explored, due to the attractiveness of the Bayesian formulation in terms of the speed of computations (sequentiality) and the possibility to take uncertainties into account (probability distributions). In particular, particle filtering was proposed as a generic tool for solving the associated state estimation problem. A detailed case study on a full scale CFB power plant was presented to illustrate the practical utility of the approach. The distributions for fuel moisture and heat transfer coefficient parameters were estimated, in order to better explain the measured flue gas oxygen and bed temperatures during a reactivity test experiment. A clear scenario was found, pointing towards a potential increasing trend in the moisture content during the tests. The involved uncertainties were made visible by plotting the quantiles of the associated distributions.

The main strengths of the approach are in that:

- both the model and the measurements are efficiently used, and that the role of the two can be transparently interpreted;

- there is a solid theory behind the bayesian state estimation;
- the parameter and state/output predictions are not limited to sample realizations, expectations, or a priori determined distributions (such as Gaussians);
- the approach is easy to implement for any simulation model (the model equations do not need to be rewritten, nor are any closed-form solutions required).

What is required is that the model can be written and simulated in a state-space form, Equations (2) and (3), i.e., given an initial state and controls, the model computes the next state and extracts the outputs.

An important strength of the approach is due to that the system state (including unknown parameters, etc.) are represented via a sample distribution. However, efficient use of this wealth of information also poses some additional challenges, as important parts of the information may be lost if only expectations or mean/variance information is monitored to the user, or fed back to system via control actions. How to illustrate sequences of multidimensional distributions in a useful way? Also the set-up of algorithm parameters may require some trial-and-error experimentation, which may be uncomfortably slow given the computational intensity of the approach.

In the filtering case, the results were briefly compared with those from using UKF, and the performance of UKF was found adequate in the examined case. Due to the smaller number of required plant model simulations, the computational load of the UKF is only a fraction of that with PF. However, using UKF in the context of the smoothing problems remains an open issue requiring further studies.

A large amount of modelling work has and is being conducted at the industry and academia to model various industrial processes. Often, the bottleneck is not in the lack of models but in how to make maximal use of the ones that already exist. The research work reported in this paper aims at extracting more out of the modelling investments, via improved understanding of the plant (model-based analysis), improved design (model tuning) and improved on-line control (design of on-line process state estimation).

REFERENCES

[1] M. Arulampalam, S. Maskell, N. Gordon and T. Clapp, A tutorial on particle filters for online/non-Gaussian Bayesian tracking, *IEEE Transactions on Signal Processing*, vol.50, no.2, pp.174-188, 2002.

[2] O. Cappé, S. Godsill and E. Moulines, An overview of existing methods and recent advances in sequential Monte Carlo, *Proc. of the IEEE*, vol.95, no.5, pp.899-924, 2007.

[3] A. Doucet, N. Freitas and N. Gordon, *Sequential Monte Carlo Methods in Practice*, Springer, Berlin, 2001.

[4] A. Doucet and A. Johansen, A tutorial on particle filtering and smoothing: Fifteen years later, *Oxford Handbook of Nonlinear Filtering*, pp.656-704, 2011.

[5] N. J. Gordon, J. Salmond and A. F. M. Smith, Novel approach to nonlinear/non-Gaussian Bayesian state estimation, *IEE Proc. of Part F: Radar and Signal Processing*, vol.140, no.2, pp.107-113, 1993.

[6] A. Haryanto, K.-S. Hong and C. Jeon, Nonlinear model predictive control of an oxy-fuel combustion boiler for regulating the excess oxygen percentage in the flue gas, *SICE Annual Conference*, Japan, 2008.

[7] A. Hotta, R. Kuivalainen, T. Eriksson, A. Sánchez-Biezma Sacristán, J. Jubitero, M. Lupion and V. Cortes, Development and demonstration of oxy-fuel CFB technology, *Industrial Fluidization Johannesburg*, South Africa, 2011.

[8] T. Hyppänen, J. Ritvanen and J. Kaikko, *Kiertoleijukattilan Dynamiikka (www-pages)*, http://www.lut.fi/fi/technology/lutenergy/energy/research/energyconversion/projects/dynamics/Sivut/Default.aspx, 2011.

[9] E. Ikonen, E. Gómez-Ramírez and K. Najim, Process regulation via genealogical decision trees, *Optimal Control Applications and Methods*, vol.30, no.2, pp.121-133, 2009.

[10] E. Ikonen and U. Kortela, Dynamic model for a bubbling fluidized-bed coal combustor, *Control Engineering Practice*, vol.2, no.6, pp.1001-1006, 1994.

[11] E. Ikonen and J. Kovács, Learning control of fluidized-bed combustion processes for power plants, in *Artificial Intelligence in Energy and Renewable Energy Systems*, S. Kalogirou (ed.), 2007.
[12] E. Ikonen, J. Kovács, H. Aaltonen, J. Ritvanen, I. Selek and A. Kettunen, Analysis and tuning of a CFB model using particle filtering, *IFAC Power Plant and Power System Control Symposium*, Toulouse, France, 2012.
[13] E. Ikonen and K. Najim, *Advanced Process Identification and Control*, Marcel Dekker, New York, 2002.
[14] E. Ikonen, I. Selek and J. Bene, Optimization of pumping schedules using the genealogical decision tree approach, *Chemical Product and Process Modeling*, vol.7, no.1, pp.1-25, 2012.
[15] R. Isermann, Model-based fault-detection and diagnosis – Status and applications, *Annual Reviews in Control*, vol.29, pp.71-85, 2005.
[16] A. Jazwinski, *Stochastic Processes and Filtering Theory*, Academic Press, 1970.
[17] T. Jäntti and K. Räsänen, Circulating fluidized bed technology towards 800 MWe Scale – Lagisza 460 Mwe supercritical CFB operation experience, *Power Gen Europe*, Milan, Italy, 2011.
[18] S. Julier and J. Uhlmann, A new extension of the Kalman filter to nonlinear systems, *Int. Symp. Aerospace/Defence Sensing, Simul. and Controls*, vol.3, 1997.
[19] A. Kettunen, T. Hyppänen, A.-P. Kirkinen and E. Maikkola, Model-based analysis of transient behavior of large-scale CFB boilers, *Proc. of the 17th International Fluidized Bed Combustion Conference*, Jacksonville, FL, USA, 2003.
[20] T. Khan, L. Udpa and S. Upda, Particle filter based prognosis study for predicting remaining useful life of steam generator tubing, *IEEE Conf. on Prognostics and Healt Management*, Lansing, USA, pp.1-6, 2011.
[21] J. Kovács, M. Hultgren, M. Jegoroff, H. Mikkonen, A. Tourunen and A. Kettunen, Comparative study on air and oxy combustion in a pilot CFB boiler, *The 21st International Conference on Fluidized Bed Combustion*, Naples, Italy, 2012.
[22] K. C. Lee, A. Oka, E. Pollakis and L. Lampe, A comparison between unscented Kalman filtering and particle filtering for RSSI-based tracking, *The 7th Workshop on Positioning, Navigation and Communication*, pp.157-163, 2010.
[23] L. Ljung and S. Söderström, *Theory and Practice of Recursive Identification*, MIT Press, 1983.
[24] R. van der Merwe, A. Doucet, N. de Freitas and E. Wan, The unscented particle filter, *Technical Report CUED/F-INFENG/TR 380*, Cambridge University Engineering Department, 2000.
[25] K. Najim, E. Ikonen and E. Gómez-Ramírez, Trajectory tracking control based on a genealogical decision tree controller for robot manipulators, *International Journal of Innovative Computing, Information and Control*, vol.4, no.1, pp.53-62, 2008.
[26] K. Najim, E. Ikonen and P. Del Moral, Open-loop regulation and tracking control based on a genealogical decision tree, *Neural Computing & Applications*, vol.15, no.3/4, pp.339-349, 2006.
[27] J. Ritvanen, J. Kovács, M. Salo, M. Hultgren, A. Tourunen and T. Hyppänen, 1-D dynamic simulation study of oxygen fired coal combustion at pilot sclae CFB boiler, *The 21st International Conference on Fluidized Bed Combustion*, Naples, Italy, 2012.
[28] D. Salmond and N. Gordon, *An Introduction to Particle Filters. Incomplete Draft*, http://www.mendeley.com/research/introduction-to-particle-filters/, 2005.
[29] A. Sankaranarayanan, A. Srivastava and R. Chellappa, Algorithmic and architechtural optimizations for computationally efficient particle filtering, *IEEE Transactions on Image Processing*, vol.17, no.5, pp.737-748, 2008.
[30] K. van Schagen, L. Rietveld, R. Babuška and E. Baars, Control of the fluidised bed in the pellet softening process, *Chemical Engineering Science*, vol.63, pp.1390-1400, 2008.
[31] J. Sjöberg, J. Q. Zhang, L. Ljung, A. Benveniste, B. Delyon, P. Glorennec, H. Hjalmarsson and A. Juditsky, Nonlinear black-box modelling in system identification: A unified overview, *Automatica*, vol.31, pp.1691-1724, 1995.
[32] N. Ukidwe, B. Bakshi and G. Parthasarathy, A multiscale Bayesian framework for designing efficient and sustainable industrial systems, *AiChE Annual Meeting*, Austin, USA, 2004.
[33] K. J. Åström and B. Wittenmark, *Adaptive Control*, Prentice-Hall, 1994.